Cell surface receptor kinase FERONIA linked to nutrient sensor TORC1 signaling controls root hair growth at low temperature in *Arabidopsis thaliana*

Javier Martínez Pacheco[1,*], Limei Song[2,*], Victoria Berdion Gabarain[1], Juan Manuel Peralta[1], Tomás Urzúa Lehuedé[3,4], Miguel Angel Ibeas[3,4], Sirui Zhu[2], Yanan Shen[2], Feng Yu[2,†] & José M. Estevez[1,3,4,†]

[1]Fundación Instituto Leloir and IIBBA-CONICET. Av. Patricias Argentinas 435, Buenos Aires C1405BWE, Argentina.
[2]State Key Laboratory of Chemo/Biosensing and Chemometrics, College of Biology, and Hunan Key Laboratory of Plant Functional Genomics and Developmental Regulation, Hunan University, Changsha 410082, P.R. China.
[3]Centro de Biotecnología Vegetal, Facultad de Ciencias de la Vida, Universidad Andres Bello.
[4]ANID - Millennium Science Initiative Program - Millennium Institute for Integrative Biology (iBio) and Millennium Nucleus for the Development of Super Adaptable Plants (MN-SAP), Santiago, Chile.

*Co-first authors.
[†]Correspondence should be addressed. Email: feng_yu@hnu.edu.cn (F.Y) and jestevez@leloir.org.ar (J.M.E).

Abstract

Root hairs (RH) are excellent model systems for studying cell size regulation since they elongate several hundred-fold their original size. Their growth is determined both by intrinsic and environmental signals. Although nutrients availability in the soil are key factors for a sustained plant growth, the molecular mechanisms underlying their sensing and downstream signaling pathways remains unclear. Here, we identified the low temperature (10°C) triggers a strong RH cell elongation response involving the cell surface receptor kinase FERONIA (FER) and the nutrient sensing role of TOR Complex 1(TORC1). We found that FER is required to perceive limited nutrients availability caused by low temperature, to interacts with and activate TORC1-downstream components to trigger RH growth. We also found that nitrate availability could mimic the RH growth response at 10°C via an unknown specific mechanism involving the NRT1.1 transceptor. Our findings reveal a new molecular mechanism by which a central hub composed by FER-TORC1 might be involved in the control of RH cell elongation under low temperature.

Abstract Word counts 164

Text Word counts 3,377
Figures 1-5
Figure S1-S3

43 **Introduction**

44

45 Root hairs (RHs) are single cells that develop as a cylindrical protrusion from the root epidermis in
46 a developmentally regulated manner. RHs are able to expand in a polar manner several hundred
47 times their original size in a couple of hours to reach water-soluble nutrients in the soil, to promote
48 interactions with the local microbiome, and to support the anchoring of the plant. RH growth is
49 controlled by the coordination of a plethora of environmental and endogenous factors[1]. Recently,
50 an autocrine mechanism of RH growth was described where RALF1-FER complex recruits and
51 phosphorylates the early translation factor eIF4E1 to enhance protein synthesis of specific mRNAs,
52 including the RH growth master regulator: *ROOT HAIR DEFECTIVE SIX-LIKE4 (RSL4)*[2]. It is known that
53 macronutrients availability are key factors that promotes rapid RH growth[1,3,4]. Although nitrate is
54 detrimental to RH growth, their mechanisms of action remain unknown[5–7] . The
55 CHLORINA1/NITRATE TRANSPORTER1.1 (CHL1/NRT1.1) was proposed as a transceptor (transporter
56 and receptor) for nitrates[8–10] as well as for auxin transport[11]. When the position T101 of NRT1.1 is
57 phosphorylated, NRT1.1 becomes a high-affinity NO_3^- (nitrate) transporter, giving this protein a
58 dual-affinity capability[12–15] . Recently, we have shown that at low temperature conditions (at 10
59 °C), nutrients availability in the media is reduced and triggers an exacerbated RH growth that is
60 suppressed if nutrients are increased[16]. Although great advances were achieved in our
61 understanding on how RH growth occurs at low temperature, it is still unclear how nutrient
62 availability derived from low temperature is perceived in the RH cells and which are the non-
63 transcriptional responses that control RH growth.

64

65 TARGET OF RAPAMYCIN (TOR) is an evolutionarily conserved Ser/Thr protein kinase in all
66 eukaryotic organisms that acts as a central growth regulator controlling metabolism and protein
67 synthesis[17–19] .TOR is found in at least two distinct multiprotein complexes called TOR Complex 1
68 and 2 (TORC1 and TORC2), although only TORC1 was experimentally validated in plants[20,21] . The
69 *Arabidopsis* TORC1 complex is encoded by one *TOR* gene (*At*TOR)[22] ,two *REGULATORY-ASSOCIATED*
70 *PROTEIN OF TOR (RAPTOR A and B)* genes[23–28], and two *LETHAL WITH SEC THIRTEEN 8 (LST8)*
71 genes[29]. In contrast to the embryo-lethal *tor*-null mutant lines, *raptor1b* and *lst8-1* mutants are
72 viable but show significant growth issues and developmental phenotypes[30]. Some canonical
73 downstream targets of TOR are conserved in plants, such as the S6 kinase (S6K) which stimulates
74 protein translation[25,31–34]. In plants, TORC1 complex plays a key role during many stages of the plant
75 life cycle by controlling both anabolic and catabolic downstream processes. In addition, TORC1 is
76 activated by nutrient availability and inactivated by stresses that alter cellular homeostasis[19,35–39].
77 The TORC1 complex senses and integrates signals from the environment to coordinate
78 developmental and metabolic processes including hormones (e.g., auxin), several nutrients (e.g.,
79 Nitrogen and Sulfur), amino acids and glucose[17,28,40–44]. However, the underlying molecular
80 mechanisms by which TORC1 operates at a single plant cell level has yet to be elucidated. Although

81 the sensing and uptake of nutrients by RHs is crucial for the plant productivity, the molecular
82 mechanisms underlying these processes remain unknown. Until now, few upstream regulators of
83 TOR have been described in plants. Among them, there is a single subfamily of Rho GTPases (ROPs)
84 involved in the spatial control of cellular processes by signaling to the cytoskeleton and vesicular
85 trafficking. Particularly, ROP2 GTPase activates TOR in response to auxin and nitrogen signals[44–46].
86 In addition, ROP2 is described as a monomeric GTP-binding protein that participates in many
87 cellular signaling processes, including the polar growth of pollen tubes and root hairs[47–50]. ROPs
88 activation is regulated by ROP guanine nucleotide exchange factors (ROP-GEFs) which interact with
89 several receptor-like kinases (RLKs) including the *Cr*RLK family member: FERONIA (FER)[48]. During
90 the cell elongation of RH, ROP2 is activated by the ROPGEF1-FER interaction. This process is also
91 regulated by ROP-GEF4 and ROP-GEF10[48,51] .Therefore, ROP2 (among other ROPs) may bridge the
92 membrane receptor FER with TORC1 activation, although this was not yet demonstrated.
93
94 FERONIA was also linked to carbon/nitrogen balance during the plant growth[52]. Even more, it was
95 shown that the cytoplasmic kinase domain of FER and its partner RIPK (RPM1-induced protein
96 kinase) interact with TOR and RAPTOR-A forming a complex to positively modulate TOR pathway
97 under nutrient starvation. Currently, it is clear that plant growth can be affected via FER-TOR axis
98 since they act early by linking amino acid and/or nutrients signaling with global protein synthesis[52].
99 Existing evidences suggest that nutrient mediated sensing at the cell surface level triggers a
100 response thought the TOR signaling pathway. However, it is still unknown which are the
101 environmental signals activated in RH by the FER-TORC1 pathway. Taking into account that
102 previously we described that a low temperature stress is able to trigger an exacerbated RH
103 growth[16,53], this stress condition was used as a proxy to investigate which are the environmental
104 signals that activate RH cell elongation. Our research reveals a novel mechanism in which FER and
105 TORC1 are necessary to regulate RH growth in *Arabidopsis* in the context of the nutrient availability
106 (nitrate) as cause of low temperature stress.
107
108
109 **Results**
110
111 **FER is required to trigger a strong RH growth response at low temperature.** Here, we asked which
112 might be the cell surface protein involved in perceiving and/or transducing the low temperature
113 stimulus. Since FER was shown as an important hub between the cell surface signaling with
114 downstream processes during RH growth[2,48] ,we tested if the *fer-4* null mutant and *fer-5* (a
115 truncated version with shortened kinase domain (KD)) are able to respond to low temperature
116 stimulus. Both *fer* mutants failed to trigger RH growth regardless the temperature (**Figure 1A**). On
117 the contrary, the related CrRLK1L ERULUS (ERU), previously linked to RH growth and cell wall
118 integrity processes with a severe short cell elongated RH phenotype at 22°C[54,55], was able to react

119 to low temperature and triggered a RH growth response although to a lower extent than Wt Col-
120 0. This indicates that FER, but not ERU, might be involved specifically in this growth response
121 despite being phylogenetically related[55] .Then, a fluorescent translational reporter line of FER
122 (FER*p*:FER-GFP), was used to study *FER* expression in RHs in two growth stages, an initial and a later
123 stage. FER is clearly activated under low temperature stimulus at the initiation stage of RH growth
124 and to a lower extent at a later stage (**Figure 1B**). Finally, phosphorylated and non-phosphorylated
125 levels of FER (FER-p/FER) were quantified at both temperatures. Under low temperature, almost
126 half of the FER protein levels was present as a non-phosphorylated form and after 3 days of growth,
127 almost all FER protein was present as a phosphorylated version (**Figure 1C**). This indicates that low
128 temperature not only increases FER protein levels in growing RHs at the plasma membrane but
129 also promotes a complete phosphorylation of FER protein, possibly enhancing the interaction with
130 putative partners and triggering the activation of downstream signaling components of RH polar
131 growth.
132
133 **TORC1 pathway is involved in low temperature induced RH growth.** Recently, it was shown that
134 FER-RIPK interacts with TOR-RAPTOR and phosphorylates it leading to the TOR pathway activation
135 in the context of nutrient perception and global metabolism regulation. We then asked if TOR might
136 be also involved in the RH growth process under low temperature. In the first place, a β-estradiol
137 (es)-induced TOR knockdown (*tor-es,* es-induced RNAi silencing of TOR) line[56] showed short RHs as
138 previously has been reported[33] and notably, a lack of response to low temperature stimulus (**Figure**
139 **2A**). Secondly, in a similar manner, inhibition of TOR kinase activity with AZD-8055[57], a novel ATP-
140 competitive inhibitor of mTOR kinase activity, abolished the RH growth at both 22°C and low
141 temperature (**Figure 2B**). On the other hand, overexpression of TOR enhanced RH growth at both
142 temperatures assayed (**Figure 2C**). These results lead us to suggest that the TOR pathway is
143 involved in the RH low temperature growth response and might operates downstream of FER. At
144 the transcriptional level, TOR expression levels are upregulated in roots up to three-folds at 10 °C
145 vs 22 °C (**Figure S1**). To deepen in this study, we tested if the growth response at low temperature
146 in RHs is also affected in mutants of the TORC1 pathway and some downstream components. All
147 the mutants *(raptor1b, rps6b,* and *lst8-1)* were all unable to respond to the low temperature
148 treatment but their RHs phenotypes showed a broad spectrum of responses in terms of cell length
149 with respect to the Wt Col-0 (**Figure 2C**). For instance, *raptor1b* behaved similarly to *tor-es* mutant,
150 while *rps6b* had an intermediate phenotype and *lst8* was comparable to Wt Col-0 (at 22°C) (**Figure**
151 **2C**). In addition, the overexpression of TOR and the S6 kinase 1 (S6K1), as a direct downstream
152 target of TOR, showed enhanced RH growth at 22 °C. Since previous reports showed that
153 phosphorylation of the ribosomal S6K1 can be used to monitor TOR protein kinase activity in
154 plants[33,56] ,we measure the ratios of S6K-p/S6K. Lower levels of S6K-p/S6K were detected for those
155 lines with strong short RH phenotype (mutants in components of the TORC1 complex and in FER
156 protein) while those with longer RHs (overexpression of S6K1 and TOR) showed higher ratios

157 (**Figure 2D, 3D**). These results clearly indicate that TORC1 and some downstream components (e.g.
158 S6K) promote RH growth under low temperature.
159
160 **FER regulates TOR polar localization in RH and activation of TORC1 pathway at low temperature.**
161 Since TORC1 activation under a plethora of stimuli usually triggers the phosphorylation of the
162 downstream factor S6K (S6K-p), we asked if low temperature responses regulated by FER might
163 control this output. With this in mind, we investigated the molecular mechanisms by which TORC1-
164 S6K are induced at 10 °C and we tested whether this might be mediated by FER. Since *fer-4* and
165 *tor-es* showed a similar RH phenotypes at low temperature (**Figure 2A-B**), possibly indicating that
166 they may act in the same pathway, we first tested if FER and TOR interaction is enhanced under
167 10°C vs 22°C. By performing a co-immunoprecipitation (Co-IP) analysis, we found that FER-TOR
168 protein-protein interaction is enhanced under low temperature (**Figure 3A**). This confirms a direct
169 interaction between FER and TOR kinase in low temperature RH mediated growth. Then, by
170 evaluating the immunolocalization of TOR in the growing RHs, we found that FER is required for
171 the apical accumulation of TOR since TOR lost the polar pattern in *fer-4* root hairs. In addition, the
172 level of RH tip-localized TOR detected was similar at both, low temperature and control conditions
173 (22°C) (**Figure 3B-C**). This indicates that in root hairs, TOR is able to localize into the tip and this is
174 dependent on FER. Then, it was tested if FER is involved in the S6K activation by TOR by measuring
175 the ratio of S6K-p/S6K proteins under both growth conditions in Wt Col-0, *fer-4*, *fer-5*, and FER^{K565R},
176 which has been shown to abolish FER autophosphorylation and transphosphorylation in an *in vitro*
177 kinase activity assay[58,59] ,although some activity might remain[60]. Interestingly, low temperature
178 enhanced S6K-p levels after 3 days of growth in Wt Col-0 at low temperature but this was partially
179 suppressed in all *fer* mutants tested (**Figure 3D**). This suggests that FER controls the level of TORC1
180 activation under low temperature in RH. Collectively, these results indicate that TOR localization in
181 the RH tip and TORC1 activation is dependent on FER and enhanced at low temperature.
182
183 **Nitrate perception and transport mediated by NRT1.1 controls RH growth at low temperature.**
184 Previous studies have been shown that nitrogen and specifically nitrates are important nutrient for
185 TOR signaling[44,61] . Since low temperature growth conditions reduce the availability of nutrients in
186 the media and trigger a strong response in RH growth[16,53] , we decided to test if nitrate signaling
187 pathway might be involved. We found that high levels of nitrate (18.8 mM) were able to repress
188 low temperature mediated RH growth while low levels of nitrate (0.5 mM) did not affect growth
189 under this temperature (**Figure 4A**). This clearly indicated that nitrate is one of the major growth
190 signals that activate RH cell elongation at low temperature where there is a low nutrient mobility
191 environment. Then, we tested if the dual affinity nitrate transporter and sensor NRT1.1 is involved
192 in this low temperature RH growth response. The NRT1.1 null mutants *chl1-5*, *chl1.9* (NRT1.1
193 harbors a substitution P492L that suppresses its root nitrate uptake activity[8] ,as well as the
194 catalytically inactive $CHL1^{T101D}$ version showed a strong RH growth response despite the

195 temperature conditions (**Figure 4B**), similarly to *S6K1-OE* and *TOR-OE* lines (**Figure 2C**), but to a
196 lower extent in terms of RH cell elongation. As expected, similar levels of S6K-p/S6K were detected
197 in the *chl1-9* line at both temperatures (**Figure 4C**). When these NRT1.1 mutants were grown under
198 high (18.8 mM) or low (0.5mM) nitrate concentrations at both temperatures (at 22°C and at 10°C),
199 a similar RH phenotype was detected between both nitrate conditions either at 22 °C or 10 °C
200 (**Figure 4D**). On the contrary, as expected Wt Col-0 RH were sensitive to both, low temperature and
201 nitrate levels. Overall, this suggested a key role of NRT1.1 in the perception of changes in nitrate
202 levels and in the regulation of the downstream TORC1-S6K activation. At this point, we
203 hypothesized that FER might be a good candidate to controls NRT1.1 activity under low
204 temperature (and low nitrate), but this remains to be tested.
205
206 **ROP2 is required for low temperature RH growth.** Previous studies have shown a key role of ROP2
207 in the regulation of RH polarity and elongation[49,62,63], as an important molecular link between FER
208 and downstream components involved in RH growth[48]. In addition, ROP2 promotes the activation
209 of TOR and its relocation to the cell periphery and induces the downstream translation pathway[45].
210 More importantly, ROP2 was shown to integrate diverse nitrogen and hormone signals for TOR
211 activation[44]. In the first place, *rop2* abolishes the differential growth responses at 10°C and
212 produces a very short RH phenotype (**Figure 5A**). While high levels of TOR are able to enhance RH
213 growth regardless of the temperature treatments (**Figure 2C**), the constitutively active ROP2
214 version (CA-ROP2) is able to repress TOR activation (**Figure 5A**). As expected, 35S-TOR-GFP (TOR
215 OE) with constitutive long RHs at both temperatures showed much higher levels of S6K-p/S6K than
216 Wt Col-0 while the presence of CA-ROP2 (in TOR OE/CA-ROP2) was able to reduce the levels of S6K-
217 p/S6K linked to a diminished RH growth (**Figure 5B**). Then, we asked if TOR partition between
218 plasma membrane/cell surface-cytoplasmic localization might be changed by the effect of low
219 temperature (equal to reduced nutrient environment) and if this is changed by the presence of CA-
220 ROP2 (**Figure 5C**). Low temperature triggers a higher cell surface TOR localization while the
221 presence of CA-ROP2 abolishes this effect. Taken together, we observed a direct effect of CA-ROP2
222 version in the TOR localization at the RH tip, RH growth responses and TORC1 activation. Then, we
223 tested if a treatment with exogenous auxin (100 nM IAA) that is able to trigger a strong RH growth
224 response and ROP2 activation, might be able to bypass silenced TOR growth inhibition effect in RH
225 at both, room and low temperatures (**Figure S2**). In this case, auxin treatment was able to partially
226 revert RH growth inhibition under TOR silenced line. Because of ROP2 activity and other possible
227 unknown effectors, auxin is able to partially rescue RH growth when TOR is inhibited, highlighting
228 that other pathway might be still being active downstream auxin independently of TORC1 to trigger
229 RH cell elongation.
230
231

232 **Discussion**

233

234 Growth and development of plants and animals are based on nutrient and hormonal signaling that
235 constitute as the main regulatory networks in eukaryotes. Unraveling the functions of the
236 regulatory hubs and their detailed molecular mechanisms are critical for understanding the
237 deepened modes of regulation in these signaling pathways. Our study uncovers a new molecular
238 mechanism by which plants use FER-ROP2-TORC1 signaling pathway to control cell elongation in
239 RH under nutrient starvation induced by low temperature stress. Here we showed that the cell
240 surface FER receptor is able to regulate TOR apical localization and further downstream activation,
241 both controlling S6K phosphorylation linked to RH growth. Based on the results obtained, here we
242 propose a model in which the FER-ROP2-TORC1 axis might be able to regulate the RH growth under
243 low temperature with remarked attention to variable nitrate conditions (**Figure S3**). It is based on
244 the mutants tested in this signaling pathway, FER-TOR enhanced interactions, TOR polar
245 localization in RHs and S6K-p/S6K as a TORC1 activation response. Changes in nitrate
246 concentrations in the media mimicked this response at low temperature and mutants on the
247 NRT1.1 transceptor are insensitive at RH growth level regardless the temperature or nitrate levels.
248 We hypothesize that low nitrate in the media might rapidly induce the levels of mature-active
249 RALF1 (and possibly other RALF peptides), which might then activate FER-ROP2-TORC1 pathway
250 and the downstream fast cell elongation effect to search for further nutrients sources. This
251 autocrine mechanism dependent on RALF1-FER growth activation has been recently demonstrated
252 for RH[2,64] ,but not in a context that involves low temperature/low nitrate and TORC1 pathway.
253 Finally, several questions in our proposed model (**Figure S3**) remain to be answered in future
254 studies. How does low nitrate concentration (low temperature) triggers FER-TORC1 activation?
255 Does RALF1 and other RALFs respond to low nitrate to activate FER? Does FER activate NRT1.1
256 directly? Recently, it was shown that FER-regulated ROP2 triggers a new mechanism for the
257 negative regulation of rhizosphere microorganisms such as *Pseudomonas*[65] .Although not tested
258 here, FER-ROP2-TORC1 signaling coupled to enhanced RH growth under low temperature (low-
259 nutrients) might be linked in root growth in specific soil conditions to select favorable microbiota
260 in the soil. This pathway may integrate complex signals from soil nutrients and microbiota in the
261 rhizosphere to plant root cell growth mechanism.

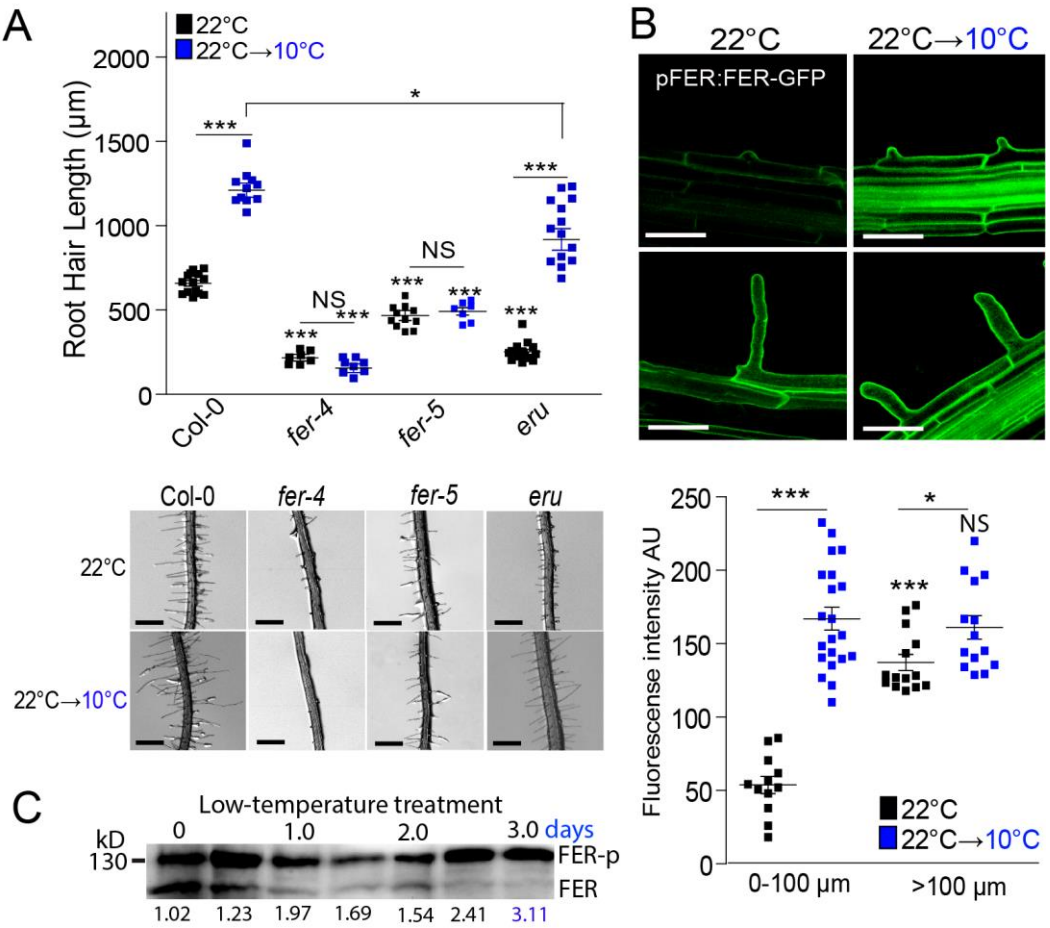

Figure 1. High levels of FER in its phosphorylated form is required to trigger the low temperature RH growth.

(A) Scatter-plot of RH length of Col-0, of *fer-4*, *fer-5*, and *eru* mutants grown at 22°C or at 10°C. RH growth is enhanced at low temperature in Wt Col-0 and *eru* mutant but not in the *fer-4* and *fer-5* mutants. Each point is the mean of the length of the 10 longest RHs identified in a single root. Data are the mean ± SD (N=10-20 roots), two-way ANOVA followed by a Tukey–Kramer test; (*) p <0.05, (***) p <0.001, NS=non-significant. Results are representative of three independent experiments. Asterisks indicate significant differences between Col-0 and the corresponding genotype at the same temperature. Representative images of each genotype are shown below. Scale bars= 500 µm. (B) Confocal images of the reporter line of FER in two growth stages of RH cells, short RHs (on top) and long RHs (on the bottom) at 22°C *vs* low temperature (10°C). Below, quantification of the GFP fluorescence intensity in RH tip. Fluorescence AU data are the mean ± SD (N=11-20 root hairs), two-way ANOVA followed by a Tukey–Kramer test; (*) p < 0.05, (***) p < 0.001. Results are representative of two independent experiments. Asterisks on the graph indicate significant differences. Scale bars: 100 µm.

278 (C) Phosphorylation levels on FER (FER-p in *p*FER:FER-GFP) increases after 3 days at low
279 temperature in roots. Phosphorylated levels of FER were analyzed by ImageJ.

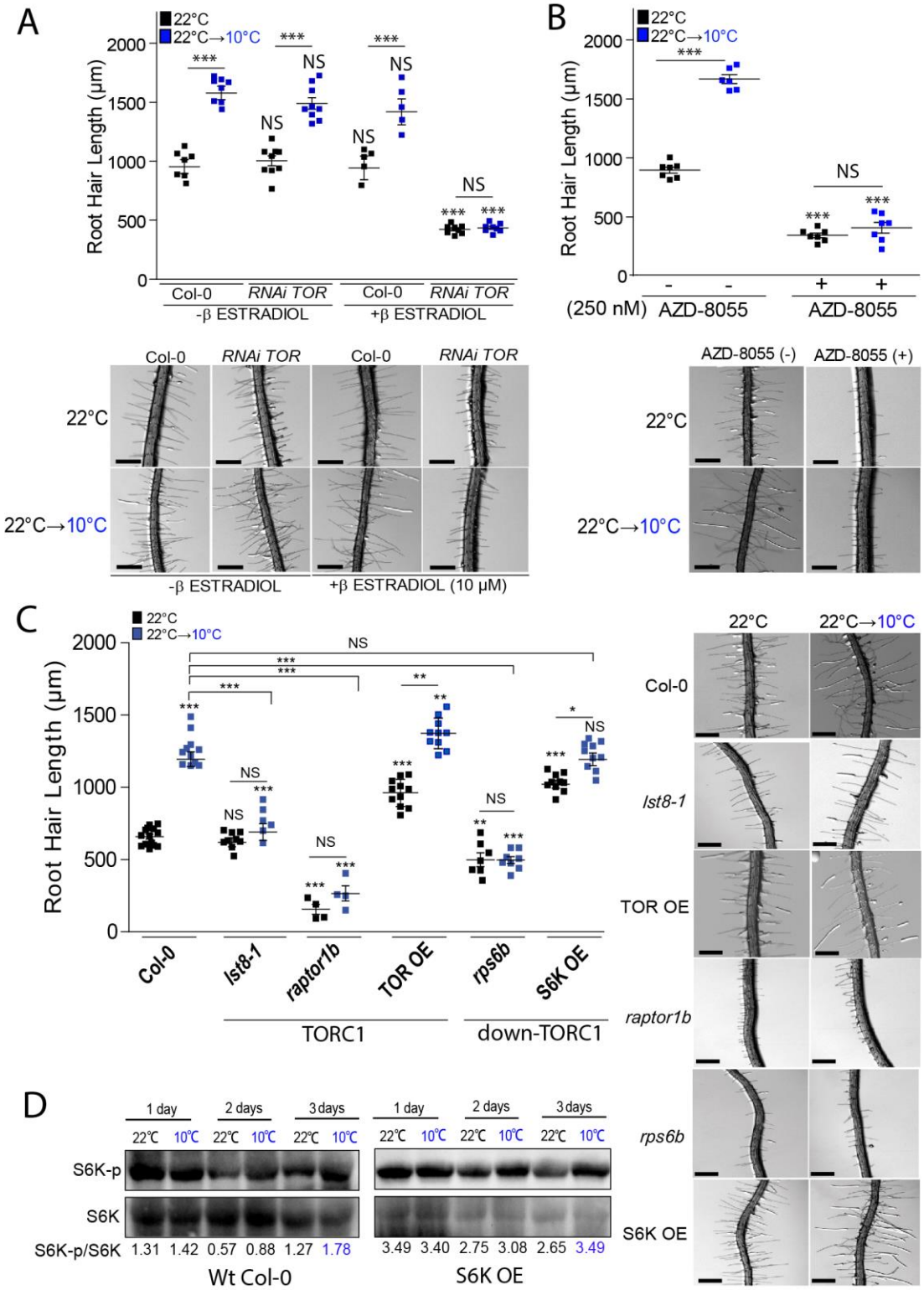

Figure 2. TORC1 signaling pathway is required for low temperature triggered RH growth.

283 (A) Scatter-plot of RH length of Col-0 and *tor-es* line grown at 22°C or at 10°C. Differential growth
284 of RH at low temperature is suppressed in the estradiol inducible *RNAi TOR* line. Each point is the
285 mean of the length of the 10 longest RHs identified in a single root. Data are the mean ± SD (N=7-
286 10 roots), two-way ANOVA followed by a Tukey–Kramer test; (***) p <0.001, NS=non-significant.
287 Results are representative of three independent experiments. Asterisks indicate significant
288 differences. Representative images of each line are shown below. Scale bars= 500 µm.
289 (B) Differential growth of RH at low temperature is abolished in the Col-0 treated with 250nM of
290 TOR inhibitor, AZD-8055. Each point is the mean of the length of the 10 longest RHs identified in a
291 single root. Data are the mean ± SD (N=7 roots), two-way ANOVA followed by a Tukey–Kramer test;
292 (***) p <0.001, NS=non-significant. Results are representative of three independent experiments.
293 Asterisks indicate significant differences. Representative images of each line are shown below.
294 Scale bars= 500 µm.
295 (C) RH cell elongation of TORC1 and downstream TORC1 signaling pathway mutants under low
296 temperature. Each point is the mean of the length of the 10 longest RHs identified in a single root.
297 Data are the mean ± SD (N=7-12 roots), two-way ANOVA followed by a Tukey–Kramer test; (*) p
298 <0.05, (**) p <0.01, (***) p <0.001, NS=non-significant. Results are representative of three
299 independent experiments. Asterisks indicate significant differences. Representative images of each
300 line are shown on the right. Scale bars= 500 µm.
301 (D) Analysis of the phosphorylation state of S6K (S6K-p/S6K ratio) in Col-0 and *S6K-OE* line. A
302 representative immunoblot is shown of a three biological replicates. S6K-p/S6K ratio was analyzed
303 by ImageJ.

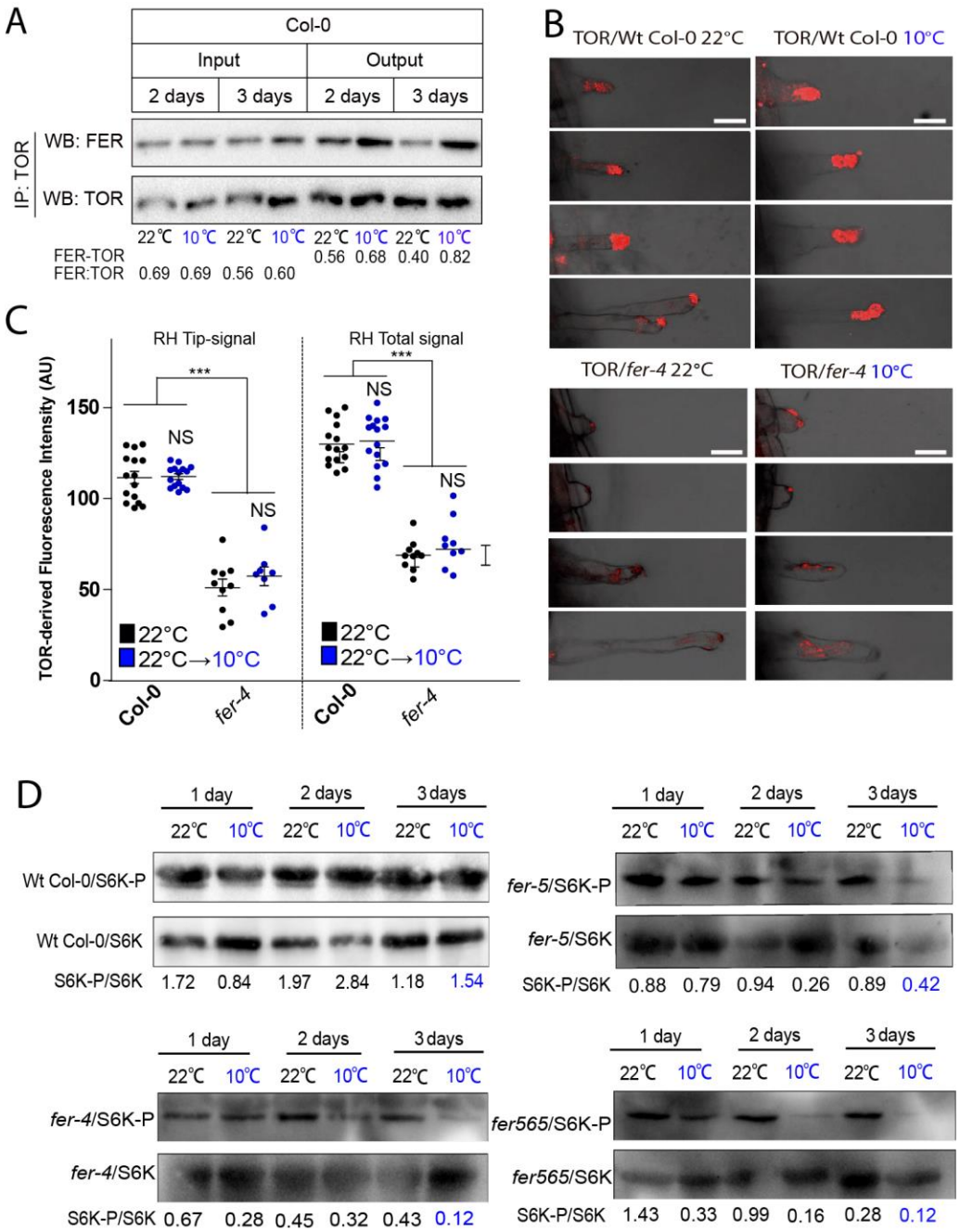

Figure 3. **FER controls apical TOR localization and subsequent activation thus increasing phosphorylation of S6K under low temperature.** (A) Enhanced FER-TOR interaction at low temperature in roots by Immunoprecipitation (IP). A representative experiment of three replicates is shown.

(B) On the top, TOR immunolocalization in RHs is FER-dependent. Scale bar=20 µm

(C) Apical and total TOR signal quantification in RHs showed in (B). A ROI at the RH tip of the fluorescent signal or all the RH TOR-derived fluorescent signal was measured. Fluorescence AU

313 data are the mean ± SD (N=10-15 root hairs), two-way ANOVA followed by a Tukey–Kramer test;
314 (***) $p < 0.001$, NS= non significant. Results are representative of two independent experiments.
315 Asterisks on the graph indicate significant differences.
316 (D) Analysis of the phosphorylation state of S6K in Wt Col-o, *fer-4, fer-5*, and *FER*^{K565R} mutants
317 Arabidopsis roots. Phosphorylation of S6K (S6K-p) is enhanced at low temperature and requires
318 FER active kinase. A representative immunoblot is shown of a three biological replicates. S6K-p/S6K
319 ratio was analyzed by ImageJ.

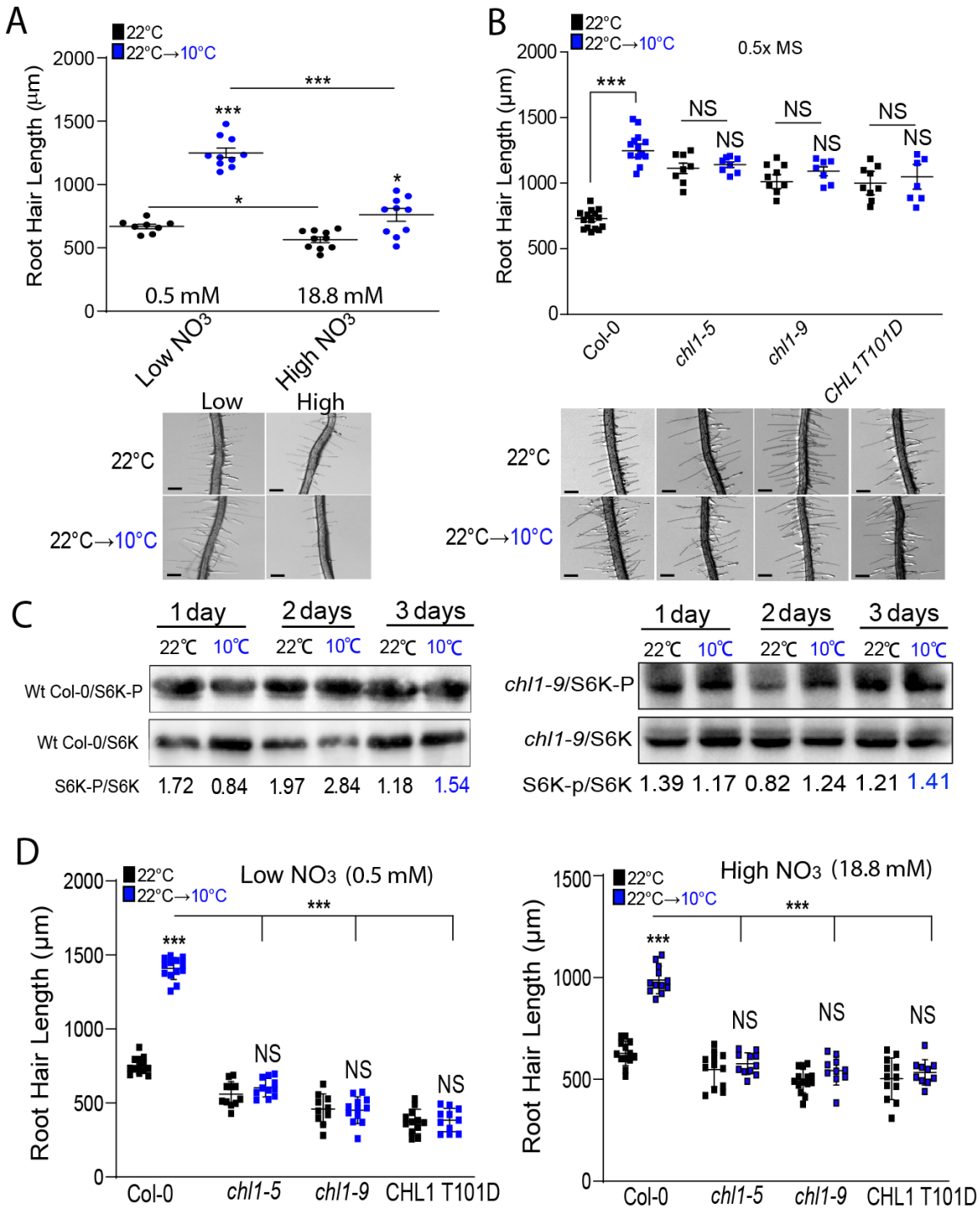

Figure 4. Nitrate acts as a RH growth signal perceived by NRT1.1 and triggered by TORC1 pathway at low temperature growth.

(A) High nitrate (18.8 mM) suppresses low temperature enhanced RH growth in Wt Col-0 plants. . Each point is the mean of the length of the 10 longest RHs identified in a single root. Data are the mean ± SD (N=10 roots), two-way ANOVA followed by a Tukey–Kramer test; (*) p <0.05, (***) p

327 <0.001. Results are representative of three independent experiments. Asterisks indicate significant
328 differences. Representative images of each line are shown below. Scale bars= 500 µm.
329 (B) Low temperature RH growth is regulated by the nitrate sensor NRT1.1 (CHL1). Scatter-plot of
330 RH length of Col-0 in low or high nitrate conditions(right); RH length of Col-0 and NRT1.1 mutants,
331 (left) grown at 22°C or 10°C. Each point is the mean of the length of the 10 longest RHs identified
332 in a single root (N=15-20). Each point is the mean of the length of the 10 longest RHs identified in
333 a single root. Data are the mean ± SD (N= 10-15 roots), two-way ANOVA followed by a Tukey–
334 Kramer test; (***) *p* <0.001, NS= non-significant. Results are representative of three independent
335 experiments. Asterisks indicate significant differences. Representative images of each line are
336 shown below. Scale bars= 500 µm.
337 (C) Analysis of the phosphorylation state of S6K in Wt Col-0 and *chl1-9* mutant roots. A
338 representative immunoblot is shown of a three biological replicates. S6K-p/S6K ratio was analyzed
339 by ImageJ.
340 (D) RH growth responses under high and low nitrate (18.8 mM and 0.5mM, respectively) in Wt Col-
341 0, *chl1-5*, *chl1-9* mutants, and $CHL1^{T101D}$ grown at 22°C or 10°C. Each point is the mean of the length
342 of the 10 longest RHs identified in a single root. Data are the mean ± SD (N= 10-15 roots), two-way
343 ANOVA followed by a Tukey–Kramer test; (***) *p* <0.001, NS= non-significant. Results are
344 representative of three independent experiments. Asterisks indicate significant differences.

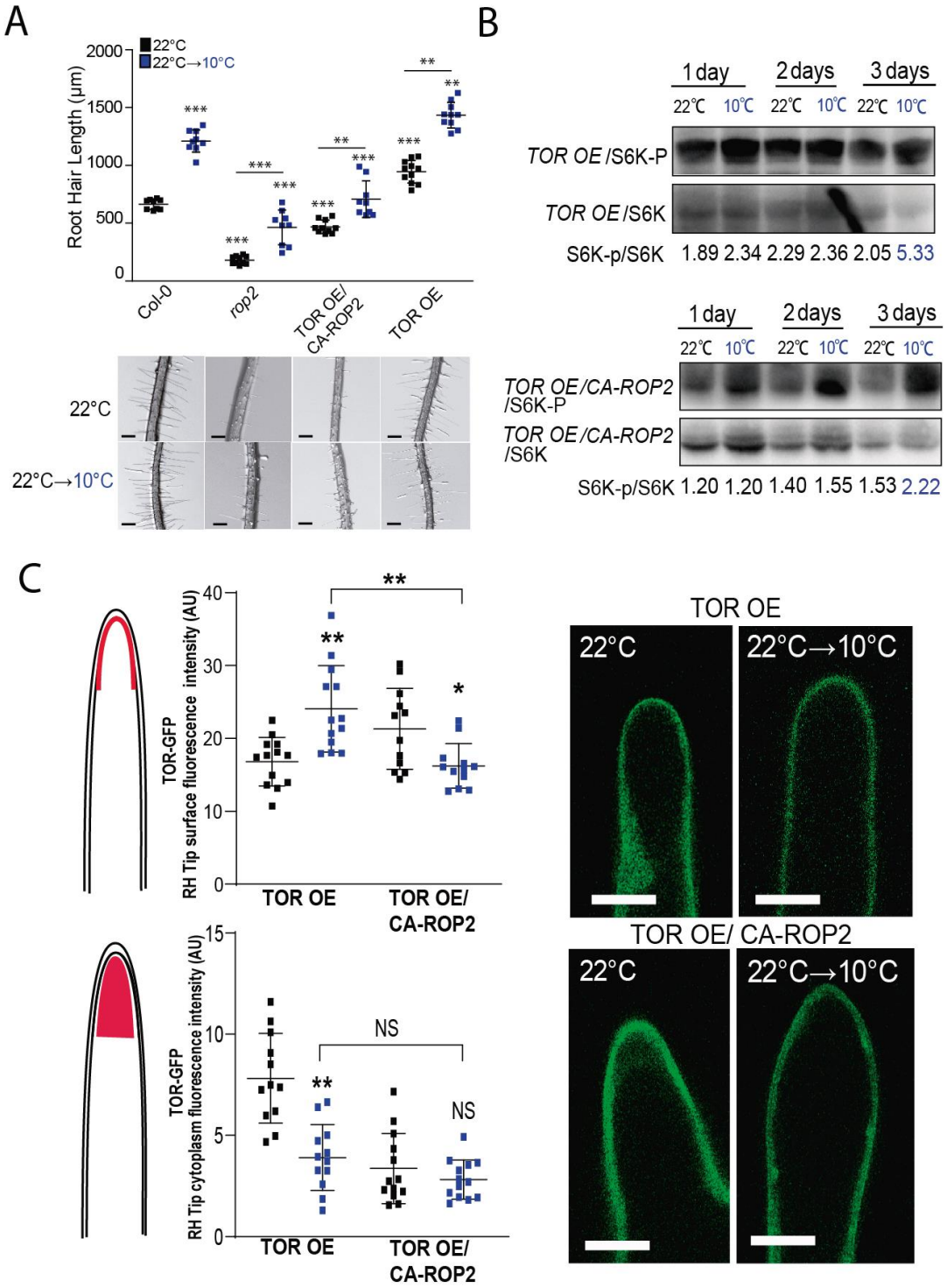

Figure 5. ROP2 is required to triggers RH growth at low temperature. (A) ROP2 is required for RH at low temperature meanwhile *rop2* and CA-ROP2/35S-TOR block RH growth. Each point is the mean of the length of the 10 longest RHs identified in a single root. Data are the mean ± SD (N= 10-15 roots), two-way ANOVA followed by a Tukey–Kramer test; (**) p <0.01, (***) p <0.001. Results

351 are representative of three independent experiments. Asterisks indicate significant differences.
352 Representative images of each line are shown below. Scale bars= 500 µm.
353 (B) Analysis of the phosphorylation state of S6K in *TOR-OE* and *TOR-OE / ROP2-CA Arabidopsis*
354 roots. Phosphorylation of S6K (S6K-p) is enhanced in *TOR-OE* and suppressed in *TOR-OE*/ROP2-CA.
355 A representative immunoblot is shown of a three biological replicates. S6K-p/S6K ratio was
356 analyzed by ImageJ.
357 (C) Quantification of TOR-GFP localization in the cell surface versus cytoplasmic localization in the
358 RH tip in Wt Col-0 and in CA-ROP2 background. Fluorescence AU data are the mean ± SD (N=12-15
359 root hairs), two-way ANOVA followed by a Tukey–Kramer test; (*) $p < 0.05$, (**) $p < 0.01$, NS= non-
360 significant. Results are representative of two independent experiments. Asterisks on the graph
361 indicate significant differences. Representative images of each line are shown on the right. Scale
362 bars= 1 µm.

363

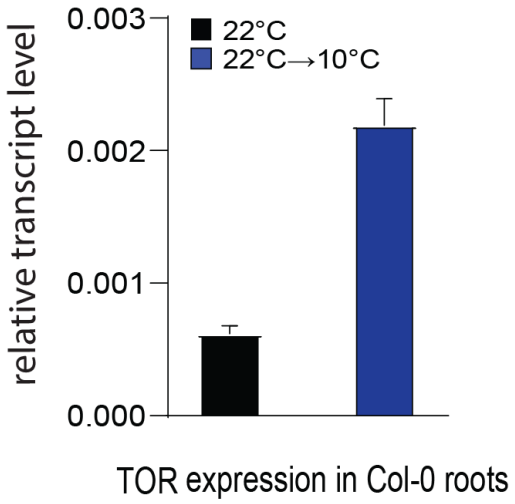

364
365

366 **Figure S1.** Quantitative PCR of *TOR* expression levels in Col-0 roots grown at 22°C and 10°C. *ACT2*
367 expression was used for normalization of gene expression. Three biological replicates and three
368 technical replicates per experiment were performed**.**

369

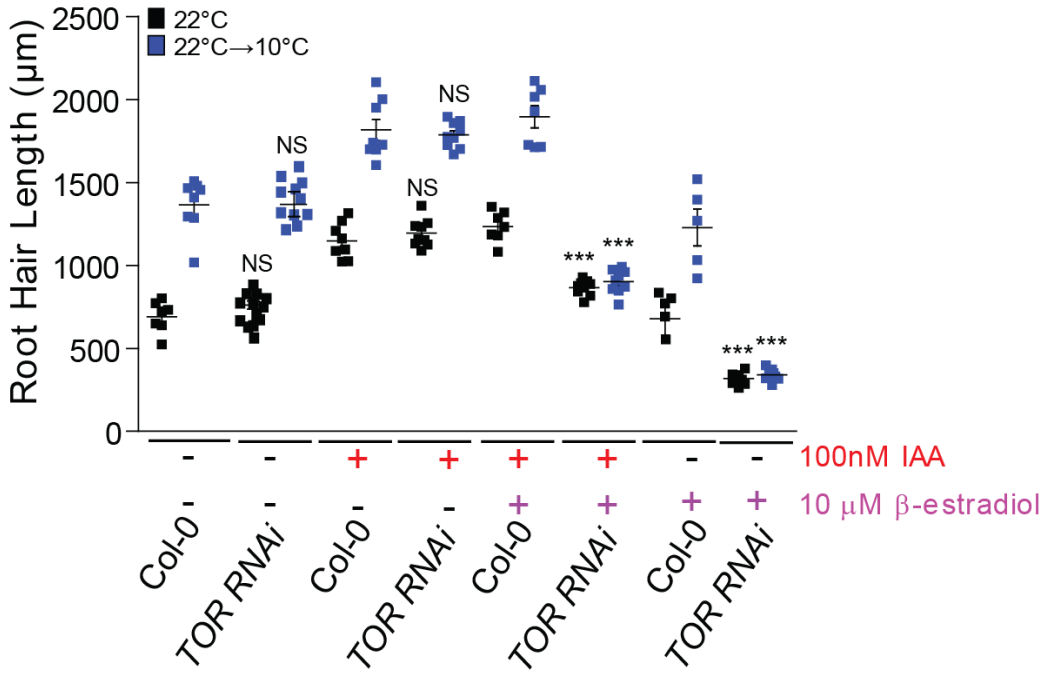

370

371

372 **Figure S2. TOR-pathway on RH growth is partially dependent on auxin.**

373 RH length of non-treated and treated Col-0 and TOR-RNA*i* line (*tor-es*) with 100nM IAA at 22°C *vs*
374 10°C. Each point is the mean of the length of the 10 longest RHs identified in a single root. Data are
375 the mean ± SD (N= 10-15 roots), two-way ANOVA followed by a Tukey–Kramer test; (***) p <0.001,
376 NS=non-significant. Results are representative of three independent experiments. Asterisks
377 indicate significant differences.

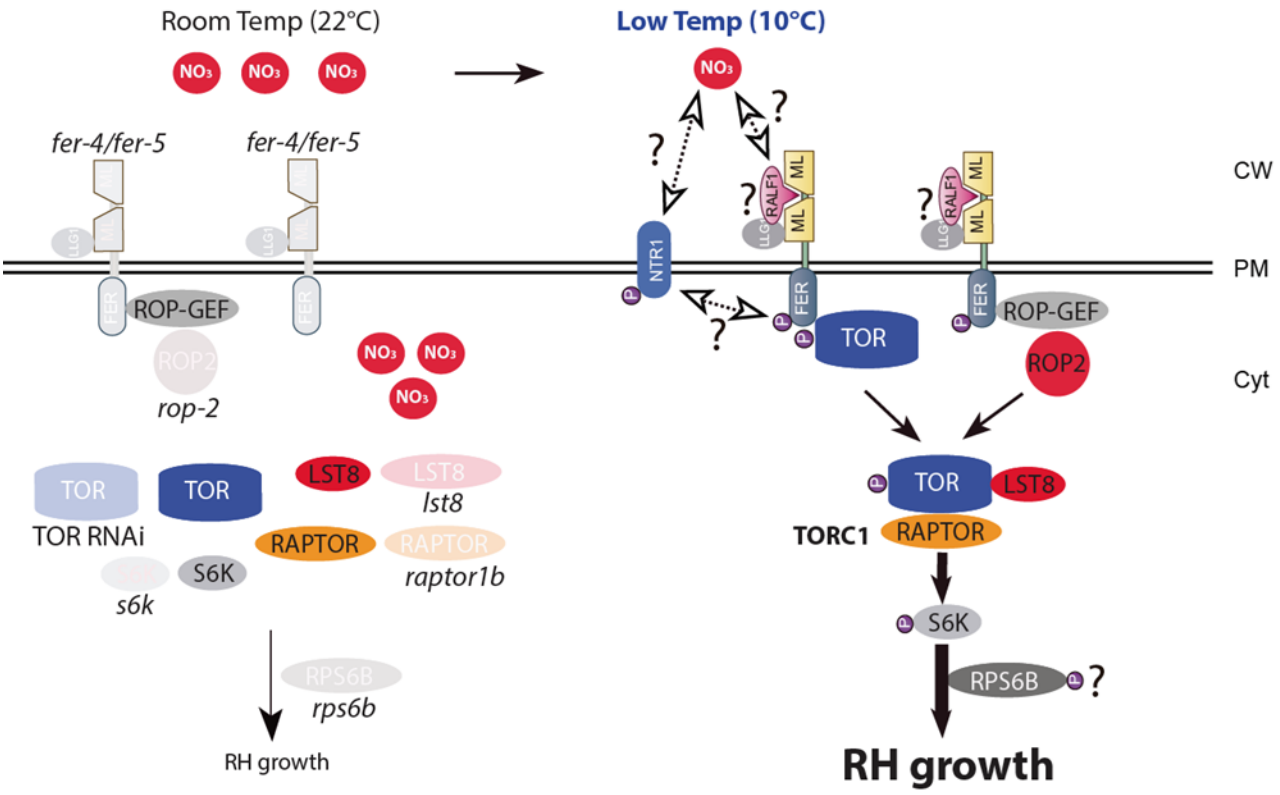

Figure S3. **Proposed model of FER-ROP2-TORC1 pathway at low temperature-nitrate that triggers cell elongation in RHs**. On the left, several mutants characterized in this work. On the right, the model based on the current evidence shown in this work and together with previous works. Low temperature triggers a low nitrate environment that leads to FER activation, enhanced FER-TOR interaction and TORC1 activation. This promotes cell elongation of RHs. This response also requires ROP2 that might bridge FER with TORC1. Several questions (?) remain to be answered in future studies such as how low nitrate (low temperature) triggers FER-TORC1 activation? Does FER activate NRT1.1 directly? Do RALF1 and other RALFs respond to low nitrate to activate FER?.

388 **Experimental Procedures**

389

390 **Root hair phenotype.** Seeds were surface sterilized and stratified in darkness for 3 days at 4°C.
391 Then grown on ½ strength MS agar plates supplemented with MES (Duchefa, Netherlands), in a
392 plant growth chamber at 22°C in continuous light (120 µmol.sec-1.m-2) for 5 days at 22°C plus 3
393 days at 10°C (moderate-low temperature treatment) or for 8 days at 22°C as control. For
394 quantitative analyses of RH phenotypes, 10 fully elongated RH from the maturation zone were
395 measured per root under the same conditions from treatment and control. Measurements were
396 made after 8 days. Images were captured using an Olympus SZX7 Zoom Stereo Microscope
397 (Olympus, Japan) equipped with a Q-Colors digital camera and Q Capture Pro 7 software (Olympus,
398 Japan). Results were expressed as the mean ± SD using the GraphPad Prism 8.0.1 (USA) statistical
399 analysis software. Results are representative of three independent experiments, each involving 7–
400 20 roots.

401

402 **Plant Material and Growth Conditions.** Plants were grown on agar plates in a plant chamber at
403 22 °C for 7 days at 24 hs light (120 µmol.seg-1.m-2). *A. thaliana* Col-0 ecotype was used as a wild-
404 type plant. A Murashige & Skoog-based media without N, P nor K (M407, PhytoTechnology
405 Laboratories, https://phytotechlab.com/) was used as the growth base medium under sterile
406 conditions. To test the low and high nitrate response, 0.5X M407 media was supplemented with
407 0.8% plant agar (Duchefa, Netherlands); 1.17mM MES,0.625 mM KH_2PO_4 monobasic and 0.5mM
408 or 18.8 mM KNO_3, respectively. Plants were treated for the indicated period in accordance with
409 prior conditions. *chl1-5*, *chl1-9 and T101D* mutants were kindly donated by Dr Yi-Fang Tsay. *tor-es*
410 was kindly donated by Dr Ezequiel Petrillo, *lst8-1*, *rps6b*, *raptor1b* and overexpressing line S6K1
411 kindly donated by Dr Elina Welchen and *35S::GFP-TOR* and *35S::GFP-TOR/CA-ROP2* kindly donated
412 by Dr. Lyubov Ryabova.

413

414 **Pharmacological Treatments.** Plants were grown on solid 0.5x MS medium plates at 22°C for 5 days
415 at 24 hs light (110 µmol.seg-1.m-2). Then transferred to plates containing solid 0.5x MS, according
416 with the specific treatment, supplemented with 100nM IAA (auxin treatment), 250nM AZD-8055
417 (TOR inhibition) or 10 µM β-estradiol (TOR RNA*i* estradiol inducible line). Treatments were
418 incubated at 22 °C for 3 days at 24 hs light (110 $\mu mol.seg^{-1}.m^{-2}$) and then at 10 °C for 3 days at 24
419 hs light (110 $\mu mol.seg^{-1}.m^{-2}$).

420

421 **Confocal Microscopy.** Confocal laser scanning microscopy for the lines *pFER::FER-GFP, 35S::GFP-*
422 *TOR and 35S::GFP-TOR/CA-ROP2*, was performed using a Zeiss LSM 710 NLO microscope (Zeiss,
423 Germany) (Excitation: 488 nm argon laser; Emission: 490-525 nm, EC Plan Neofluar 40X/1.3 Oil or
424 a Zeiss Plan-Apochromat 63X/1.4 Oil objectives). GFP signal at the cell surface and cytoplasm of the
425 RH tip were quantified using ROIs with the ImageJ software. Fluorescence AU were expressed as

426 the mean ± SD using the GraphPad Prism 8.0.1 (USA) statistical analysis software. Results are
427 representative of two independent experiments, each involving 10–15 roots and approximately,
428 between 10 to 20 hairs per root were observed.
429
430 **Co-IP assay**. For Co-IP assays using A/G agarose and an anti-TOR antibody[33], 30 µL of A/G beads
431 (Thermo Fisher Scientific Inc., 20421) was resuspended and washed three times using NEB buffer
432 (20 mM HEPES [pH 7.5], 40 mM KCl, 5 mM $MgCl_2$) before adding 8 µL of anti-TOR antibody or
433 preimmune serum as a negative control [33] in a total volume of 500 µL of NEB buffer, followed by
434 incubation for 4 h at 4 ˚C. Col-0 seedlings were first grown at 22 ˚C for 5 days then transferred to
435 22 ˚C or 10 ˚C for 2 days or 3 days. For protein extraction from plants, the collected materials were
436 ground to a fine powder in liquid nitrogen and solubilized with NEB-T buffer (20 mM HEPES [pH
437 7.5], 40 mM KCl, 5 mM $MgCl_2$, 0.5% Triton X-100) containing 1 × protease inhibitor cocktail (Thermo
438 Fisher Scientific Inc., 78430) and 1 × phosphatase inhibitor (Thermo Fisher Scientific Inc., 78420)
439 and incubated for 1 h on the ice. The extracts were centrifuged at 16,000 g at 4 ˚C for 15 min, and
440 the resultant supernatant was incubated with prepared antibody-beads from the above step. After
441 overnight incubation at 4 ˚C with rotation, the agarose beads were washed five times with the NEB
442 buffer and eluted with elution buffer (0.2 M glycine, 0.5% Triton X-100, pH 7.5). Anti-FER and anti-
443 TOR antibodies[33] were used for immunoblotting to detect the immunoprecipitates.
444
445 **TOR immunolocalization**. Col-0 and *fer-4* seedlings were first grown at 22 ˚C for 4 days before
446 transferred to 22 ˚C or 10 ˚C for 2 days and treatment with or without 1 µM RALF1 for 30min. Then
447 seedlings were collected and incubated for 10 min under vacuum (0.05 MPa) in phosphate-
448 buffered saline (PBS) containing 4% paraformaldehyde and 0.1% Triton X-100. Seedlings were
449 washed gently three times (10 min for each wash) in PBS and then the cell wall was digested in 2%
450 Driselase (Sigma, D8037) in PBS for 18 min at 37 ˚C and washed five times with PBS. The
451 permeability of the seedlings was increased by incubating them in 3% IGEPAL CA-630 (Sigma,
452 18896) and 10% DMSO in PBS for 18 min, followed by washed three times with PBS. Seedlings were
453 incubated in 2% bovine serum albumin (BSA) (Ameresco, 0332) in PBS for 1.5 h and then incubated
454 with primary TOR antibody[33] (antibody diluted 1:600 in 2% BSA) for overnight at 4 ˚C. The seedlings
455 were washed with PBS for five times. Fluorophore-labeled secondary antibody (goat–mouse
456 secondary antibody, diluted 1:600 in 2% BSA) was incubated with the samples at 37 ˚C for 5 h in
457 the dark. Seedlings were washed five times with PBS before observation. Fluorescent signal
458 detection and documentation were performed using a Nikon confocal laser scanning microscope
459 with a 560-nm band-pass filter for IF555 detection.
460
461 **S6K-P/S6K immunoblotting detection.** For immunological detection of S6K-P and S6K1/2, total
462 soluble proteins were extracted from 50 mg of plant materials grown as indicated previously with
463 100 µL 2 × Laemmli buffer supplemented with 1% Phosphatase Inhibitor Cocktail 2 (Thermo Fisher

464 Scientific Inc., 78430). Proteins were denatured for 10 min at 95 ˚C and separated on 10% or 8%
465 SDS-PAGE. Rabbit *At*TOR polyclonal antibodies (Abiocode, R2854-2), rabbit polyclonal S6K1/2
466 antibodies (Agrisera, AS121855), and S6K1-p (phospho T449) antibody (Abcam, ab207399) were
467 used for immunoblotting.
468
469 **Quantitative PCR (qPCR).** Total root RNA was extracted from plantlets grown *in vitro* at 22 ˚C and
470 10 ˚C using the RNeasy®Plant Mini Kit (QIAGEN, Germany). One microgram of total RNA was
471 reverse transcribed using an oligo$(dT)_{20}$ primer and the Super Script™ IV RT (Invitrogen,USA)
472 according to the manufacturer's instructions. cDNA was diluted 20-fold before PCR. *q*PCR was
473 performed on a LightCycler®480 Instrument II (Roche, USA) using 2 µL of 5X HOT
474 FIREPol®EvaGreen® qPCR Mix Plus(no ROX) (Solis BioDyne, Estonia), 2 µL of cDNA, and 0.25 µM of
475 each primer in a total volume of 10 µL per reaction. ACT2 (AT3G18780) gene was used as reference
476 for normalization of gene expression levels (ACT2 primers, F: GGTAACATTGTGCTCAGTGGTGG R:
477 CTCGGCCTTGGAGATCCACATC; TOR primers, F: GAAGATGAAGATCCCGCTGA R:
478 GCATCTCCAAGCATATTTACAGC[45]). The cycling conditions were: 95 °C for 12 min., 35 cycles of 95 °C
479 for 15 sec., 60 °C for 1 min. and finally a melting curve from 60 °C to 95 °C (0.05°/sec). Data were
480 analyzed using the $\Delta\Delta C_t$[66] method and LightCycler®480 Software, version 1.5 (Roche). Two
481 independent experiments with three biological and three technical replicates per experiment,
482 were performed.

Acknowledgements

We would like to thank Elina Welchen, Ezequiel Petrillo, Lyubov A. Ryabova, Yi-Fang Tsay, Kriss Vissenberg for the seed lines. We thank NASC (Ohio State University) for providing T-DNA lines seed lines. J.M.E. is investigator of the National Research Council (CONICET) from Argentina. M.I. is supported by ANID FONDECYT POSTDOCTORADO [grant 3220138]. This work was supported by grants Natural Science Foundation of China (NSFC-32001974 and NSFC-31871396) to F.Y. and from ANPCyT (PICT2017-0066, and PICT2019-0015), by ANID – Programa Iniciativa Científica Milenio ICN17_022, NCN2021_010 and Fondo Nacional de Desarrollo Científico y Tecnológico [1200010] to J.M.E.

Author Contribution

J.M.P performed most of the experiments, analysed the data and helped in the writing process of the manuscript. L.S. performed the S6K-p determinations, IP of TOR-FER and immunolocalization assay of TOR. V.B.G., J.M.P., T.U.I., M.A.I., S-Z., Y.S., helped in the data analysis and writing process of the manuscript. F.Y. designed research and analysed part of the data and J.M.E. designed research, analysed the data, supervised the project, and wrote the paper. All authors commented on the results and the manuscript. This manuscript has not been published and is not under consideration for publication elsewhere. All the authors have read the manuscript and have approved this submission.

Competing financial interest

The authors declare no competing financial interests. Correspondence and requests for materials should be addressed to F.Y. (feng_yu@hnu.edu.cn) and J.M.E. (Email: jestevez@leloir.org.ar).

506 **REFERENCES**

507 1. Vijayakumar, P., Datta, S. & Dolan, L. ROOT HAIR DEFECTIVE SIX-LIKE4 (RSL4) promotes
508 root hair elongation by transcriptionally regulating the expression of genes required for cell
509 growth. *New Phytol.* **212**, 944–953 (2016).
510 2. Zhu, S. *et al.* The RALF1–FERONIA Complex Phosphorylates eIF4E1 to Promote Protein
511 Synthesis and Polar Root Hair Growth. *Mol. Plant* (2020) doi:10.1016/j.molp.2019.12.014.
512 3. Yi, K., Menand, B., Bell, E. & Dolan, L. A basic helix-loop-helix transcription factor controls
513 cell growth and size in root hairs. *Nat. Genet.* **42**, 264–267 (2010).
514 4. Datta, S., Prescott, H. & Dolan, L. Intensity of a pulse of RSL4 transcription factor synthesis
515 determines Arabidopsis root hair cell size. *Nat. Plants* **1**, 1–6 (2015).
516 5. Vatter, T., Neuhäuser, B., Stetter, M. & Ludewig, U. Regulation of length and density of
517 Arabidopsis root hairs by ammonium and nitrate. *J. Plant Res.* **128**, 839–848 (2015).
518 6. Canales, J., Contreras-López, O., Álvarez, J. M. & Gutiérrez, R. A. Nitrate induction of root
519 hair density is mediated by TGA1/TGA4 and CPC transcription factors in Arabidopsis
520 thaliana. *Plant J.* **92**, 305–316 (2017).
521 7. Liu, B., Wu, J., Yang, S., Schiefelbein, J. & Gan, Y. Nitrate regulation of lateral root and root
522 hair development in plants. *Journal of Experimental Botany* vol. 71 4405–4414 (2020).
523 8. Ho, C. H., Lin, S. H., Hu, H. C. & Tsay, Y. F. CHL1 Functions as a Nitrate Sensor in Plants. *Cell*
524 **138**, 1184–1194 (2009).
525 9. Gojon, A., Krouk, G., Perrine-Walker, F. & Laugier, E. Nitrate transceptor(s) in plants. *J. Exp.*
526 *Bot.* **62**, 2299–2308 (2011).
527 10. Bouguyon, E. *et al.* Multiple mechanisms of nitrate sensing by Arabidopsis nitrate
528 transceptor NRT1.1. *Nat. Plants* **1**, 15015 (2015).
529 11. Krouk, G. *et al.* Nitrate-regulated auxin transport by NRT1.1 defines a mechanism for
530 nutrient sensing in plants. *Dev. Cell* **18**, 927–937 (2010).
531 12. Liu, K.-H. & Tsay, Y.-F. Switching between the two action modes of the dual-affinity nitrate
532 transporter CHL1 by phosphorylation. *EMBO J.* **22**, 1005–13 (2003).
533 13. Forde, B. G. & Walch-Liu, P. Nitrate and glutamate as environmental cues for behavioural
534 responses in plant roots. *Plant, Cell Environ.* **32**, 682–693 (2009).
535 14. Léran, S. *et al.* A unified nomenclature of nitrate transporter 1/peptide transporter family
536 members in plants. *Trends in Plant Science* vol. 19 5–9 (2014).
537 15. Wang, W., Hu, B., Li, A. & Chu, C. NRT1.1s in plants: Functions beyond nitrate transport. *J.*
538 *Exp. Bot.* **71**, 4373–4379 (2020).
539 16. Moison, M. *et al.* The lncRNA APOLO interacts with the transcription factor WRKY42 to
540 trigger root hair cell expansion in response to cold. *Mol. Plant* **14**, 937–948 (2021).
541 17. Xiong, Y. & Sheen, J. The role of target of rapamycin signaling networks in plant growth and
542 metabolism. *Plant Physiol.* **164**, 499–512 (2014).
543 18. Dobrenel, T. *et al.* The arabidopsis TOR kinase specifically regulates the expression of
544 nuclear genes coding for plastidic ribosomal proteins and the phosphorylation of the
545 cytosolic ribosomal protein S6. *Front. Plant Sci.* **7**, 1–16 (2016).
546 19. Saxton, R. A. & Sabatini, D. M. mTOR Signaling in Growth, Metabolism, and Disease. *Cell*
547 **168**, 960–976 (2017).
548 20. Tatebe, H. & Shiozaki, K. Evolutionary Conservation of the Components in the TOR

549 Signaling Pathways. *Biomolecules* **7**, 1–17 (2017).
550 21. Van Leene, J. *et al.* Capturing the phosphorylation and protein interaction landscape of the
551 plant TOR kinase. *Nat. Plants* **5**, 316–327 (2019).
552 22. Menand, B. *et al.* Expression and disruption of the Arabidopsis TOR (target of rapamycin)
553 gene. *Proc. Natl. Acad. Sci. U. S. A.* **99**, 6422–6427 (2002).
554 23. Anderson, G. H., Veit, B. & Hanson, M. R. The Arabidopsis AtRaptor genes are essential for
555 post-embryonic plant growth. *BMC Biol.* **3**, 1–12 (2005).
556 24. Deprost, D., Truong, H. N., Robaglia, C. & Meyer, C. An Arabidopsis homolog of
557 RAPTOR/KOG1 is essential for early embryo development. *Biochem. Biophys. Res.*
558 *Commun.* **326**, 844–850 (2005).
559 25. Mahfouz, M. M., Kim, S., Delauney, A. J. & Verma, D. P. S. Arabidopsis TARGET of
560 RAPAMYCIN interacts with RAPTOR, which regulates the activity of S6 kinase in response to
561 osmotic stress signals. *Plant Cell* **18**, 477–490 (2006).
562 26. Yang, H. *et al.* MTOR kinase structure, mechanism and regulation. *Nature* **497**, 217–223
563 (2013).
564 27. Rexin, D., Meyer, C., Robaglia, C. & Veit, B. TOR signalling in plants. *Biochem. J.* **470**, 1–14
565 (2015).
566 28. Salem, M. A., Li, Y., Wiszniewski, A. & Giavalisco, P. Regulatory-associated protein of TOR
567 (RAPTOR) alters the hormonal and metabolic composition of Arabidopsis seeds, controlling
568 seed morphology, viability and germination potential. *Plant J.* **92**, 525–545 (2017).
569 29. Moreau, M. *et al.* Mutations in the Arabidopsis homolog of LST8/GβL, a partner of the
570 target of Rapamycin kinase, impair plant growth, flowering, and metabolic adaptation to
571 long days. *Plant Cell* **24**, 463–481 (2012).
572 30. McCready, K., Spencer, V. & Kim, M. The Importance of TOR Kinase in Plant Development.
573 *Front. Plant Sci.* **11**, 1–7 (2020).
574 31. Henriques, R. *et al.* Arabidopsis S6 kinase mutants display chromosome instability and
575 altered RBR1-E2F pathway activity. *EMBO J.* **29**, 2979–2993 (2010).
576 32. Ahn, C. S., Han, J. A., Lee, H. S., Lee, S. & Pai, H. S. The PP2A regulatory subunit Tap46, a
577 component of the TOR signaling pathway, modulates growth and metabolism in plants.
578 *Plant Cell* **23**, 185–209 (2011).
579 33. Xiong, Y. & Sheen, J. Rapamycin and glucose-target of rapamycin (TOR) protein signaling in
580 plants. *J. Biol. Chem.* **287**, 2836–2842 (2012).
581 34. Patrick, R. M. *et al.* Discovery and characterization of conserved binding of eIF4E 1 (CBE1),
582 a eukaryotic translation initiation factor 4E– binding plant protein. *J. Biol. Chem.* **293**,
583 17240–17247 (2018).
584 35. Xiong, Y. & Sheen, J. Novel links in the plant TOR kinase signaling network. *Curr. Opin. Plant*
585 *Biol.* **28**, 83–91 (2015).
586 36. Dobrenel, T. *et al.* TOR Signaling and Nutrient Sensing. *Annu. Rev. Plant Biol.* **67**, 261–285
587 (2016).
588 37. González, A. & Hall, M. N. Nutrient sensing and TOR signaling in yeast and mammals .
589 *EMBO J.* **36**, 397–408 (2017).
590 38. Bakshi, A., Moin, M., Madhav, M. S. & Kirti, P. B. Target of rapamycin, a master regulator of
591 multiple signalling pathways and a potential candidate gene for crop improvement. *Plant*

592 *Biology* vol. 21 190–205 (2019).
593 39. Pacheco, J. M. *et al.* The tip of the iceberg: emerging roles of TORC1, and its regulatory
594 functions in plant cells. *J. Exp. Bot.* **72**, 4085–4101 (2021).
595 40. Dong, Y. *et al.* Sulfur availability regulates plant growth via glucose-TOR signaling. *Nat.*
596 *Commun.* **8**, 1–10 (2017).
597 41. Cao, P. *et al.* Homeostasis of branched-chain amino acids is critical for the activity of TOR
598 signaling in Arabidopsis. *Elife* **8**, 1–24 (2019).
599 42. Schaufelberger, M. *et al.* Mutations in the Arabidopsis ROL17/isopropylmalate synthase 1
600 locus alter amino acid content, modify the TOR network, and suppress the root hair cell
601 development mutant lrx1. *J. Exp. Bot.* **70**, 2313–2323 (2019).
602 43. Sun, X. *et al.* Low nitrogen induces root elongation via auxin-induced acid growth and
603 auxin-regulated target of rapamycin (TOR) pathway in maize. *J. Plant Physiol.* **254**, 153281
604 (2020).
605 44. Liu, Y. *et al.* Diverse nitrogen signals activate convergent ROP2-TOR signaling in
606 Arabidopsis. *Dev. Cell* **56**, 1283-1295.e5 (2021).
607 45. Schepetilnikov, M. *et al.* GTP ase ROP 2 binds and promotes activation of target of
608 rapamycin, TOR , in response to auxin . *EMBO J.* **36**, 886–903 (2017).
609 46. Li, X. *et al.* Differential TOR activation and cell proliferation in Arabidopsis root and shoot
610 apexes. *Proc. Natl. Acad. Sci. U. S. A.* **114**, 2765–2770 (2017).
611 47. Carol, R. J. *et al.* A RhoGDP dissociation inhibitor spatially regulates growth in root hair
612 cells. *Nature* **438**, 1013–1016 (2005).
613 48. Duan, Q., Kita, D., Li, C., Cheung, A. Y. & Wu, H. M. FERONIA receptor-like kinase regulates
614 RHO GTPase signaling of root hair development. *Proc. Natl. Acad. Sci. U. S. A.* **107**, 17821–
615 17826 (2010).
616 49. Kang, E. *et al.* The microtubule-associated protein MAP18 affects ROP2 GTPase activity
617 during root hair growth. *Plant Physiol.* **174**, 202–222 (2017).
618 50. Denninger, P. *et al.* Distinct RopGEFs Successively Drive Polarization and Outgrowth of
619 Root Hairs. *Curr. Biol.* **29**, 1854-1865.e5 (2019).
620 51. Huang, G. Q. *et al.* Arabidopsis RopGEF4 and RopGEF10 are important for FERONIA-
621 mediated developmental but not environmental regulation of root hair growth. *New*
622 *Phytol.* **200**, 1089–1101 (2013).
623 52. Xu, G. *et al.* FERONIA phosphorylates E3 ubiquitin ligase ATL6 to modulate the stability of
624 14-3-3 proteins in response to the carbon/nitrogen ratio. *J. Exp. Bot.* **70**, 6375–6388
625 (2019).
626 53. Pacheco, J. M. *et al.* The lncRNA APOLO and the transcription factor WRKY42 target
627 common cell wall EXTENSIN encoding genes to trigger root hair cell elongation. *Plant*
628 *Signal. Behav.* **16**, 1920191 (2021).
629 54. Kwon, T., Alan Sparks, J., Liao, F. & Blancaflor, E. B. Erulus is a plasma membrane-localized
630 receptor-like kinase that specifies root hair growth by maintaining tip-focused cytoplasmic
631 calcium oscillations[OPEN]. *Plant Cell* vol. 30 1173–1177 (2018).
632 55. Schoenaers, S. *et al.* The Auxin-Regulated CrRLK1L Kinase ERULUS Controls Cell Wall
633 Composition during Root Hair Tip Growth. *Curr. Biol.* **28**, 722-732.e6 (2018).
634 56. Xiong, Y. *et al.* Glucose-TOR signalling reprograms the transcriptome and activates

635 meristems. *Nature* **496**, 181–186 (2013).
636 57. Montané, M. H. & Menand, B. ATP-competitive mTOR kinase inhibitors delay plant growth
637 by triggering early differentiation of meristematic cells but no developmental patterning
638 change. *J. Exp. Bot.* **64**, 4361–4374 (2013).
639 58. Escobar-Restrepo, J. M. *et al.* The Feronia receptor-like kinase mediates male-female
640 interactions during pollen tube reception. *Science (80-.).* **317**, 656–660 (2007).
641 59. Haruta, M., Sabat, G., Stecker, K., Minkoff, B. B. & Sussman, M. R. A peptide hormone and
642 its receptor protein kinase regulate plant cell expansion. *Science (80-.).* **343**, 408–411
643 (2014).
644 60. Chakravorty, D., Yu, Y. & Assmann, S. M. A kinase-dead version of FERONIA receptor-like
645 kinase has dose-dependent impacts on rosette morphology and RALF1-mediated stomatal
646 movements. *FEBS Lett.* **592**, 3429–3437 (2018).
647 61. Deprost, D. *et al.* The Arabidopsis TOR kinase links plant growth, yield, stress resistance
648 and mRNA translation. *EMBO Rep.* **8**, 864–870 (2007).
649 62. Jones, M. A. *et al.* The arabidopsis Rop2 GTPase is a positive regulator of both root hair
650 initiation and tip growth. *Plant Cell* **14**, 763–776 (2002).
651 63. Gendre, D. *et al.* Rho-of-plant activated root hair formation requires arabidopsis YIP4a/b
652 gene function. *Dev.* **146**, (2019).
653 64. Zhu, S., Martínez Pacheco, J., Estevez, J. M. & Yu, F. Autocrine regulation of root hair size
654 by the RALF-FERONIA-RSL4 signaling pathway. *New Phytol.* **227**, 45–49 (2020).
655 65. Song, Y. *et al.* FERONIA restricts Pseudomonas in the rhizosphere microbiome via
656 regulation of reactive oxygen species. *Nat. Plants* **7**, 644–654 (2021).
657 66. Livak, K. J. & Schmittgen, T. D. Analysis of relative gene expression data using real-time
658 quantitative PCR and the 2-ΔΔCT method. *Methods* **25**, 402–408 (2001).